Emission and absorption cross section of thulium doped silica fibers

Søren Dyøe Agger and Jørn Hedegaard Povlsen

Research Center COM, Technical University of Denmark
2800 Kgs. Lyngby, Denmark.
as@com.dtu.dk

Abstract: A thorough investigation of the emission and absorption spectra of the ($^3F_4$,$^3H_6$) band in thulium doped silica fibers has been performed. All the basic parameters of thulium in silica have been extracted with the purpose of further analysis in laser and amplifier simulations. The experimental methods used to obtain the scaled cross sections have been carefully selected in order to avoid problems associated with calibrated measurements and knowledge of the radiative lifetime. The values of the absorption cross sections agree well with previously reported values, however the peak emission to peak absorption cross section ratios are found to be significantly below 1. Also confinement factors and thulium concentrations are estimated from the results.

References and links

1. D. E. McCumber, "Theory of phonon-terminated optical masers," Phys. Rev. A **134**, A299–A306 (1964).
2. W. J. Miniscalco and R. S. Quimby, "General procedure for the analysis of Er^{3+} cross sections," Opt. Lett. **16**, 258–260 (1991).
3. M. J. F. Digonnet, E. Murphy-Chutorian, and D. G. Falquier, "Fundamental limitations of the McCumber Relation Applied to Er-doped Silica and other Amorphous-Host lasers," IEEE J. Quantum Electron. **38**, 1629–1637 (2002).
4. P. C. Becker, N. A. Olsson, and J. r. Simpson, *Erbium-Doped Fiber Amplifiers - Fundamentals and Technology* (Academic Press, 1999).
5. S. D. Jackson and S. Mossman, "Efficiency dependence on the Tm^{3+} and Al^{3+} concentrations for Tm^{3+}-doped silica double-clad fiber lasers," Appl. Opt. **42**, 2702–2707 (2003).
6. R. D. Muro, S. J. Wilson, N. E. Jolley, B. S. Farley, A. Robinson, and J. Mun, "A new method to determine the Er-fibre gain coefficient from dynamic gain tilt technique," Optical fiber communication conf. **2**, 108–110 (1999).
7. M. J. F. Digonnet, *Rare-Earth-Doped Fiber Lasers and Amplifiers* (Marcel Dekker, 2001).
8. M. Hellsing, M. Fokine, A. Claesson, L. E. Nilsson, and W. Margulis, "ToF-SIMS imaging of dopant diffusion in optical fibers," Appl. Surf. Sci. **203-204**, 648–651 (2003).
9. H. Zech, "Measurement Technique for the Quotient of Cross Sections $\sigma_e(\lambda_s)/\sigma_a(\lambda_s)$ of Erbium-Doped Fibers," IEEE Photonics Technol. Lett. **7**, 986–988 (1995).
10. W. L. Barnes, R. I. Laming, E. J. Tarbox, and P. R. Morkel, "Absorption and Emission Cross Section of Er^{3+} Doped Silica Fibers," IEEE J. Quantum Electron. **27**, 1004–1010 (1991).
11. S. D. Jackson and T. A. King, "Theoretical Modeling of Tm-Doped Silica Fiber Lasers," J. Lightwave Techn. **17**, 948–956 (1999).
12. X. Zou and H. Toratani, "Spectroscopic properties and energy transfer in Tm^{3+} singly- and Tm^{3+}/Ho^{3+} doubly-doped glasses," J. Non-crystalline Solids **195**, 113–124 (1996).
13. B. M. Walsh and N. P. Barnes, "Comparison of Tm:ZBLAN and Tm:silica fiber lasers;Spectroscopy and tunable pulsed laser operation around 1.9 μm," Appl. Phys. B **78**, 325–333 (2004).

14. H. W. Gandy, R. J. Ginther and J. F. Weller, "Stimulated emission of Tm^{3+} radiation in silicate glass," J. Appl. Phys. **36**, 3030–3031 (1967).

1. Introduction

Modeling rare-earth doped fiber amplifiers and lasers is an important task in understanding and designing new devices. A model requires detailed knowledge of the particular rare-earth which can be found from spectroscopic measurements and calculations. The extracted data are applied to numerical or analytical models to predict gain, lasing threshold, noise properties and other parameters of interest. This has been done with great success in erbium/ytterbium doped amplifiers and lasers, based on numerous investigations of the spectroscopic properties of those rare-earths when incorporated into silica fibers.

In order to have optical amplification at wavelengths other than at the erbium/ytterbium bands, other rare-earths are doped into the optical fibers. In particular, the $^3F_4 \rightarrow {}^3H_6$ transition of thulium-doped silica has the potential to cover a broad wavelength range beyond that of erbium from 1.6 μm to 2.1 μm and the spectroscopic parameters have to be accurately determined in order to model new devices. Applications of thulium-doped fiber lasers and amplifiers are spectroscopy, lidar, medicine and future communication systems. The work presented here describes the determination of lifetime, cross-sections and rare-earth concentration from in-fiber measurements of thulium doped silica. The goal of the study is to provide new and accurate spectroscopic data for modeling thulium-doped devices similar to what is known in the case of erbium/ytterbium device modeling.

Thulium doped silica fibers have in many cases similar properties to erbium doped fibers and may be modeled using the same formalism. Nevertheless, as the $^4I_{13/2} \rightarrow {}^4I_{15/2}$ transition in erbium can be considered 100 % radiative, this is far from the case with the $^3F_4 \rightarrow {}^3H_6$ transistion of thulium. This complicates the scaling of the emission cross section, since the integrated emission cross section spectrum is proportional to the radiative lifetime, only. The other posibility of scaling is to use the McCumber relation[1, 2, 3], but this method has been shown to have limitations for broad linewidths that are mainly homogenously broadened which is the case for the emission spectrum of thulium covering more than 400 nm. Finally, Judd-Ofelt analysis can be used to recover the radiative lifetime from absorption measurements, but accuracy has been shown to be limited and it requires a calibrated measurement of the emission spectrum [4].

2. Spectroscopy

A sample from a custom designed thulium doped silica fiber from OFS Fitel Denmark was available. Co-doping with aluminum and lanthanide in the core was chosen to optimize the radiative efficiency and minimize clustering [5]. Furthermore, an Al/Ge co-doped fiber was available (Tm2). The rare-earth concentration in the fibers were unknown from fabrication.

The following section describes how the spectroscopic data are recovered from simple measurements of lifetime, saturated fluorescence, ground-state absorption and gain tilt [6].

2.1. Lifetimes

The fluorescent (or observed) lifetime, τ_{fl} is a given by the radiative ,τ_r, and the non-radiative ,τ_{nr}, lifetimes as

$$\frac{1}{\tau_{fl}} = \frac{1}{\tau_r} + \frac{1}{\tau_{nr}}. \tag{1}$$

The fluorescent lifetime can be measured from a simple fluorescent decay experiment in which the $^3H_4$ level of thulium is excited by a pump diode laser at a wavelength of 786 nm. The ions
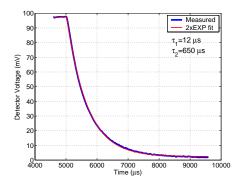
Fig. 1. Fluorescence decay from a 2 mm long fiber (Tm1) excited by a step pump power at $\lambda_p = 786$ nm along with a fitted double exponential.

excited to the $^3H_4$ level quickly relaxes to the $^3F_4$ level from where it relaxes partly radiatively to the ground state $^3H_6$. The fluorescence observed is proportional to the population of the $^3F_4$ level which decays exponentially with a lifetime of τ_{fl}. A measured curve of the fluorescence is shown in Fig. 1. The decay curve is least squares fitted to a double-exponential to recover a lifetime of 650 μs for Tm1 and 560 μs for Tm2 for the $^3F_4$ level. The lifetimes found are in good agreement with previous reported lifetimes which range from 300 to 600 μs [7].

2.2. Scaling of the absorption cross-section

Scaling of the absorption cross section is possible with knowledge of the concentration of rare-earths and the ground-state-absorption per unit length $GSA = 2\pi\sigma_a \int \rho \phi_s^2 r dr$, where ρ is the concentration and ϕ_s is the normalized mode profile of the fiber. However, as the concentration of the particular fibers in our work was unknown from the beginning, this method was ruled out. Nevertheless, once the fluorescent lifetime is known, it is possible to scale the absorption cross section even without knowledge of the rare-earth concentration. This is possible since the inversion is independent of the concentration. The inversion of a 2-level system in a short piece of fiber where the pump power is much higher than any signal power is given by

$$x(r) = \frac{N_2(r)}{N_1(r) + N_2(r)} = \frac{\sigma_{ap} n_p \phi_p^2(r)}{\sigma_{ap} n_p \phi_p^2(r)(\eta_p + 1) + \frac{1}{\tau_{fl}}}, \tag{2}$$

where σ_{ap} is the pump absorption cross section, ϕ_p is the optical mode of the pump, n_p is the pump photon current and $\eta_p = \sigma_{ep}/\sigma_{ap}$ is the ratio of emission-to-absorption cross section at the pump wavelength. The ion populations of the upper and lower laser levels are N_2 and N_1, respectively. The z-dependency of the light propagating in the fibers positive direction is given by the small signal gain and fluorescence by

$$\frac{dn_s}{dz} = 2\pi \int_0^\infty \rho(r)\{[x(r)\sigma_{es} - (1-x(r))\sigma_{as}]n_s\phi_s^2(r) + 2x(r)\sigma_{es}\}r dr, \tag{3}$$

where σ_{es}, σ_{as} are the emission and absorption cross sections at the signal wavelength.

In the following, the rare-earth distribution is assumed proportional to the refractive index profile, $\Delta n(r)$, as $\rho(r) = \rho_0 \Delta n(r)/max(\Delta n)$, ρ_0 being the peak concentration . The refractive index profile is known from measurements on both fibers and the mode profile is found numerically using a cylindrical 1D Finite-Element modesolver. This defines a confinement factor Γ
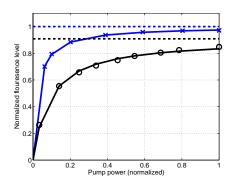
Fig. 2. Fluorescence levels generated by pumping at $\lambda_p = 786$ nm (blue +) and 1600 nm (black o) with the individual saturation levels indicated. Also shown are the fitting curves. The fiber is 2 mm of Tm1.

as

$$\Gamma = 2\pi \int_0^\infty \frac{\Delta n}{max(\Delta n)} \phi_n^2 r dr, \tag{4}$$

where Δn is the refractive index step of the fiber core relative to the cladding. The justification of doing so is found in that the index raising dopants are added along with the rare-earth dopants and that the diffusion processes are somewhat similar for the modifiers and rare-earths added [8].

Using this and assuming that the inversion is transversally independent, then Eq. (3) can be written as

$$\frac{dn_s}{dz} = \rho_0 \Gamma [(x\sigma_{es} - (1-x\sigma_{as}))n_s + 2x\sigma_{es}], \tag{5}$$

where the first term is the gain term and the second term is the spontaneous emission term. The gain term in Eq. (5) can be neglected if the fiber length is short. The fluorescence can be used to determine η_p for an in-band wavelength λ_p through measurement of the ratio of generated fluorescence to the fluorescence level generated by pumping at a wavelength where full inversion can be reached [9]. Thus pumping at $\lambda_p = 786$ nm and $\lambda_p = 1600$ nm and observing the fluorescence from a short piece of fiber at an optimum wavelength results in the curve shown in Fig. 2. First, the cross section ratio η_p is found by the ratio of the extrapolated fluorescence levels at infinite pump power for the pump wavelengths 786 nm and 1600 nm. Then, the fluorescence levels are scaled and along with values of the launched pump power fitted to Eq. (2), where the fitting parameter is σ_{ap}.

Following this procedure, the ratio of cross sections at $\lambda_p = 1600$ nm is found to be $\eta_p = 0.10 \pm 0.02$ (Tm1) and $\eta_p = 0.15 \pm 0.02$ (Tm2) from the extrapolated levels at infinite pump power. This number is then used in Eq. (2) along with values of the launched pump powers and fluorescent lifetime to fit the generated saturated fluorescence to the spontaneous emission term in Eq. (3) and thereby obtain a value of $\sigma_a = 3.5 \pm 0.1 \times 10^{-25}$ m^2 for Tm1 and $\sigma_a = 4.3 \pm 0.1 \times 10^{-25}$ m^2 for Tm1 at a wavelength of $\lambda_p = 1600$ nm.

As the absorption cross section is now known at λ_p, then the absorption cross section for all other wavelengths in the band can be found from a GSA measurement. The GSA is simplified using the confinement factor as $GSA(\lambda) = \rho_0 \sigma_a(\lambda) \Gamma(\lambda)$. This relation gives

$$\sigma_a(\lambda) = \sigma_a(\lambda_p) \frac{GSA(\lambda)}{GSA(\lambda_p)} \frac{\Gamma(\lambda_p)}{\Gamma(\lambda)}, \tag{6}$$

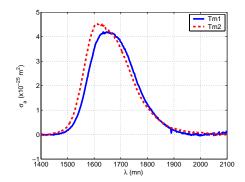from which the absorption spectra are calculated and shown in Fig. 3

Fig. 3. Absorption cross section of the Tm1 and Tm2 fiber.

2.3. Scaling of the emission cross-section

With the knowledge of the absorption cross section and $\eta(\lambda_p)$ at one wavelength, it is possible to scale the emission cross section, if the emission spectrum can be measured. However, this is not an easy task, since the measurement equipment has to be calibrated from 1.6 μm to 2.1 μm in order for the real emission spectrum to appear from a fluorescence measurement. Alternatively, one may use the factor $\sigma_a \exp(-h\nu/k_bT)$ from the McCumber relation to get the emission spectral shape, but as σ_a is very small for wavelengths beyond 1.9 μm and with the short-comings of the McCumber theory in mind, this is also problematic. To overcome this, a relative measurement of the emission spectrum is necessary and this is accomplished by measuring the gain tilt [6].

The difference in gain of a small signal passing through a rare-earth doped fiber for two different mean inversions is found from Eq. (5) to be (ignoring contribution from ASE)

$$\sigma_g = \ln \frac{n_s(L)}{n_s(0)}_{<x_1>} - \ln \frac{n_s(L)}{n_s(0)}_{<x_2>} = GSA(\eta_s + 1) < \Delta x >, \tag{7}$$

where $\eta_s = \frac{\sigma_{es}}{\sigma_{as}}$ is the signal cross section ratio and $< \Delta x >=< x_1 > - < x_2 >$ is some mean inversion. If the ratio of cross sections η_s is known for one wavelength λ', it is possible to take the ratio of Eq. (7) to obtain the emission cross section as

$$\sigma_{es} = \sigma_a(\lambda')(\eta(\lambda') + 1)\frac{\sigma_g(\lambda)}{\sigma_g(\lambda')} - \sigma_a(\lambda) \tag{8}$$

Since the ratio of emission to absorption cross section is only known at 1600 nm, which is in the low-end of the emission spectrum, it provides poor accuracy for the entire spectrum. High power pumps were not readily available at higher wavelengths, so instead of measuring the fluorescence ratios as above, it was decided to make a small signal gain measurement instead. To improve the accuracy, the gain measurement was performed at $\lambda = 1740$ nm by pumping at 786 nm and extrapolating the ratio of max. gain to the GSA for a given length L to give the ratio of cross sections [10]. A number of accurate measurements were performed at different lengths and results were reproducible to provide a result of $\eta(1740 \text{ nm}) = 1.20 \pm 0.02$ for Tm1 and 1.25 ± 0.02 for Tm2. The scaled emission cross sections then follows from Eq. (8) and are shown in Fig. 4 and 5 together with their respective absorption cross sections.

The disadvantage of the gain tilt method is that it cannot give the correct emission spectrum where there is signal Excited-State Absorption (ESA). Excited-state absorption was present for
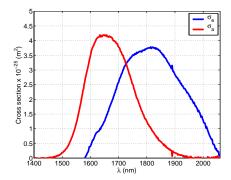
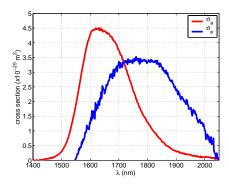Fig. 4. Absorption- and emission cross section of the Tm1-fiber.

Fig. 5. Absorption- and emission cross section of the Tm2-fiber.

the ($^3F_4$,$^3H_6$) band of the two fibers for wavelengths below 1550 nm and above wavelengths of 2065 nm. Nevertheless, in the important central region of the emission spectrum, the gain tilt method works well.

The peak absorption cross section has been reported in [11] to be 4.5×10^{-25} m^2, which is in good agreement with the value found here of 4.2 and 4.5×10^{-25} m^2. On the other hand, peak emission cross sections reported in [11],[12],[13] for thulium in silica have values of 6.0×10^{-25} m^2, 6.1×10^{-25} m^2 and 4.6×10^{-25} m^2, respectively. This is in contrast to the values obtained here of only 3.5 and 3.9×10^{-25} m^2, which agrees better with the value found in [14] of 4.0×10^{-25} m^2. The radiative lifetime in [11] was estimated from multi-phonon decay rates used to scale the cross sections. The emission cross section in [12] was found by applying the McCumber relation to the absorption cross section and scaling by comparison to a measured emission spectrum lineshape of a bulk sample. In [13], the fluorescence spectrum was measured in a preform sample and scaled by the Judd-Ofelt calculated radiative lifetime. The large discrepancy is unclear at the moment, but could be caused by measurements obtained in different samples using different methods to achieve the radiative lifetimes and emission spectrums. An overview table summarizing the above values are given in table 1.

It is seen that the absorption cross section values reported are in reasonably good agreement, whereas the peak emission cross section values seem to be either around 4×10^{-25} m^2 or 6×10^{-25} m^2. As the emission cross section values found in this study rely on the well-agreed absorption cross section values and small signal gain measurements for all in-band wavelengths,

Table 1. Spectroscopic parameters for Tm^{3+} doped silica for the $(^3F_4, ^3H_6)$ transition found in this work along with previously reported values. Values in small italic are estimated from relevant data or graphs in the references.

Media	$\sigma_{a,peak}$ ($\times 10^{-25}$ m^2)	$\sigma_{e,peak}$ ($\times 10^{-25}$ m^2)	τ_r (ms)	ref #
SM fiber	4.2-4.4	3.5-3.9	6.0-6.6	
Fiber	4.5	6.0	*4.2*	11
Bulk	-	6.1	6.3	12
Preform	*4.3*	4.6	4.56	13
Bulk	-	4.0	-	14

the uncertainty in the other methods are avoided thus providing accurate results.

The scaled emission cross section allows the calculation of the radiative lifetime through the relation

$$\frac{1}{\tau_r} = 8\pi n^2 c \int \frac{\sigma_e}{\lambda^4} d\lambda, \tag{9}$$

which gives a radiative lifetime of 6.0 ms and 6.6 ms for Tm1 and Tm2 respectively. Radiative lifetimes reported using Judd-Ofelt theory in [12] and [13] are 6.3 ms and 4.56 ms, which agrees fairly well with the values obtained here. The radiative quantum efficiency of this laser level in thulium-doped silica fibers is therefore only around 10%. The low efficiency is a well-known problem associated with the high phonon energy of silica and the relatively low energy difference between the ground- and first excited-state of thulium.

2.4. Rare-earth concentration

The last parameter to be determined is the rare-earth peak concentration, ρ_0, which is now easily obtained by the relation

$$\rho_0 = \frac{GSA}{\sigma_a \Gamma} \tag{10}$$

The concentration is hereby estimated to be approximately 8.4×10^{25} 1/m^3 for fiber Tm1 and 6.1×10^{25} 1/m^3 for fiber Tm2. The difference in concentration primarily originates from the definition of the confinement factor and that the concentration profile is assumed to follow the index distribution. The ratio of confinement factors for the two fibers is 0.7.

The order of magnitude of the estimated concentration in the fiber was also verified by comparing it to that of an erbium-doped fiber. All fiber parameters of the erbium-doped fiber, including co-doping, was the same as those for the Tm1-fiber, the only difference being that the erbium concentration was known to be approximately 11 times lower than the thulium concentration. The exact same procedure and measurements were carried out on the erbium doped fiber to estimate its concentration. The absorption cross section of the erbium fiber at a wavelength of 1470 nm was estimated to 1.24×10^{-25} m^2 using a cross section ratio at this wavelength of 0.22. Since the GSA was measured to 0.63 1/m, the concentration of the erbium doped fiber was found to be around 8.7×10^{24} 1/m^3, which is 9.5 times lower than in the thulium concentration in fiber Tm1. This result verifies the methods used to obtain all the necessary information in order the calculate the rare-earth concentration of the fibers.

3. Discussion

The most important underlying assumption in the results obtained above is that it is possible to reach full inversion, when pumping the thulium doped fiber into the $^3H_4$-excited state, i.e. at a

pump wavelength around 786 nm. This means that the cross section ratio, η_p is assumed equal to zero as in the case of erbium pumped at 980 nm. Moreover, the assumption is also that the $^4H_6$ lifetime is comparatively shorter than the lifetime of the $^3F_4$-level, such that the system is effectively a two-level system. The lifetime of the $^3H_4$-level has not been measured directly at this stage and the only information is from the double exponential fit as shown in Fig. 1, which is not very accurate. However, the estimated value is close to the reported lifetimes which range from 14 to 20 μs. From the relation $(1 + \tau_{32}/\tau_{21})^{-1}$, a maximum obtainable inversion is around 0.97 in the thulium doped fibers and the approximation is therefore believed to be reasonably good.

Another issue is ion clustering, but it is believed to be small, since the lifetimes observed are among the longest reported and the thulium concentrations are fairly modest. However, Energy-Transfer Upconversion (ETU) is present when pumping at 786 nm, which is observed by a faint blue glow from the pumped fiber. Two ions initially pump excited to the ($^3H_4, ^3H_4$) levels may exchange energy and promote into the states ($^3F_4, ^1G_4$) from where a radiative decay is possible from the $^1G_4$ to the ground state through emission of a photon at approximately 470 mn. However, the fluorescence observed at 1850 nm from a short piece of fiber, which is directly proportional to the inversion level, was never seen to decrease with increasing pump power, this being the case even at pump powers above 500 mW. Furthermore, the measured blue emission coming from the fiber was relatively small, thus justifying a low influence from this ETU process.

Even though it is not correct to assume full inversion in any rare-earth doped system, it is still believed to be a good approximation which will fall within the general uncertainty range of the measured values.

4. Conclusion

All spectroscopic parameters of the ($^3F_4, ^3H_6$) transition of a thulium doped Al/La-silica and Al/Ge-silica fiber have been obtained using simple and well-known techniques in analyzing rare-earth doped fibers. The parameters determined are based on numerous experimental measurements, thus avoiding the limitations of theoretical calculations. The results are readily usable for analyzing thulium doped silica fiber amplifiers and lasers providing the opportunity of future insight and device optimization.

Acknowledgment